ACS OMEGA

http://pubs.acs.org/journal/acsodf

Article

First Iridium(IV) Chloride–Dimethyl Sulfoxide Complex $[H(dmso)_2][IrCl_5(dmso\text{-}\kappa O)]$: Synthesis and Structure along with Novel Polymorph Modifications of $[H(dmso)_2][trans\text{-}IrCl_4(dmso\text{-}\kappa S)_2]$ and $[H(dmso)][trans\text{-}IrCl_4(dmso\text{-}\kappa S)_2]$

Olga V. Rudnitskaya,* Tatiana A. Tereshina, Ekaterina V. Dobrokhotova, Ekaterina K. Kultyshkina, Natalia A. Chumakova, Alexander I. Kokorin, Yan V. Zubavichus, and Victor N. Khrustalev*

Cite This: *ACS Omega* 2023, 8, 20569–20578

Read Online

ACCESS | Metrics & More | Article Recommendations | Supporting Information

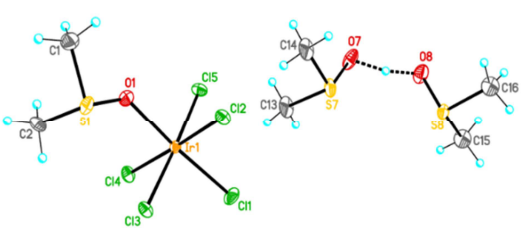

The novel iridium(IV) chloride-dimethyl sulfoxide salt **[H(dmso)$_2$][IrCl$_5$(dmso-κO)]**

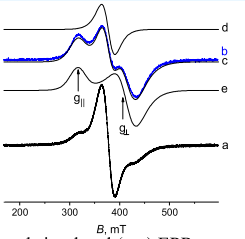

Experimental (**a**, **b**) and simulated (c-e) EPR spectra of $H_2IrCl_6 \cdot 6H_2O$ solutions in acetone – $[IrCl_6]^{2-} \rightarrow [IrCl_5(Me_2CO)]^-$ conversion

ABSTRACT: As evidenced by UV–Vis and EPR spectroscopies, the reaction of $H_2IrCl_6 \cdot 6H_2O$ or $Na_2[IrCl_6] \cdot nH_2O$ with DMSO results in a slow reduction of Ir(IV) avoiding the formation of Ir(IV) dimethyl sulfoxide complexes in measurable quantities. More specifically, we successfully isolated and solved the crystal structure of a sodium hexachloridoiridate(III), $Na_3[IrCl_6] \cdot 2H_2O$, as a product of $Na_2[IrCl_6] \cdot nH_2O$ reduction in an acetone solution. Furthermore, it was shown that $[IrCl_5(Me_2CO)]^-$ species is gradually formed in an acetone solution of $H_2IrCl_6 \cdot 6H_2O$ upon storage. The reaction of DMSO with aged acetone solution of $H_2IrCl_6 \cdot 6H_2O$ dominated by $[IrCl_5(Me_2CO)]^-$ affords a novel iridium(IV) chloride-dimethyl sulfoxide salt $[H(dmso)_2][IrCl_5(dmso\text{-}\kappa O)]$ (**1**). The compound was characterized by various spectroscopies (IR, EPR, UV–Vis) and X-ray diffraction techniques applied both to single-crystal and polycrystalline powder. The DMSO ligand is coordinated to the iridium site via the oxygen atom. New polymorph modifications of known iridium(III) complexes $[H(dmso)_2][trans\text{-}IrCl_4(dmso\text{-}\kappa S)_2]$ and $[H(dmso)][trans\text{-}IrCl_4(dmso\text{-}\kappa S)_2]$ were isolated and structurally elucidated as byproducts of the above reaction.

INTRODUCTION

Transition metal complexes bearing dimethyl sulfoxide as a ligand have been in the focus of intense studies since the mid-1990s. Compounds of that class are known for next to all metals, including platinum metals (hereinafter, PMs).[1−4]

Iridium-derived chloride–dimethyl sulfoxide complexes were described for the very first time about 50 years ago.[5] To date, a number of iridium(I) and iridium(III) chloride–dimethyl sulfoxide complexes are known. In particular, *trans*- and *cis*-isomers of $[Ir^{III}Cl_4(dmso)_2]^-$, $[mer\text{-}Ir^{III}Cl_3(dmso)_3]$, $[cis\text{-}Ir^{I}Cl_2(dmso)_2]^-$, and $[Ir^{I}Cl(dmso)_3]$ have been elucidated structurally.[6−11] Notwithstanding, no iridium(IV) chloride–dimethyl sulfoxide complex has been reported so far.

It is well known that bound through sulfur DMSO is a π-acceptor and stabilizes lower oxidation states (hereinafter, o.s.) of PMs. As it occurs frequently, the entrance of the DMSO ligands into the coordination sphere of a PM in an initial o.s. +4 is accompanied by the reduction of the PM ion to the o.s. +3 or even +2. And it is the DMSO molecule that acts as a reducing agent.

Coordination compounds containing hexachloridoiridate-(IV) ions $[IrCl_6]^{2-}$, e.g., hexachloridoiridic acid hexahydrate $H_2IrCl_6 \cdot 6H_2O$, are often applied as synthetic precursors for the variety of iridium(IV)-based chlorine-containing complexes. The $[IrCl_6]^{2-}$ anion is capable of facile reduction to $[IrCl_6]^{3-}$, thus acting as an one-electron oxidating agent. Solvents present in the system often act as coupled reducing agents for this process. Taking these arguments into account, the mere possibility of existence and preparative isolation of iridium(IV)

Received: February 15, 2023
Accepted: May 11, 2023
Published: May 27, 2023

chloride−dimethyl sulfoxide complexes has remained a subject of debate.

Processes occurring in aqueous and hydrochloric acid solutions of $[IrCl_6]^{2-}$ were the subject of several studies applying an assortment of experimental techniques.[12−17] Similar studies on the behavior of hexachloridoiridate(IV) anions in organic solvents are by far more scarce. In alcohols, the $[IrCl_6]^{2-}$ anions undergo a slow reduction to $[IrCl_6]^{3-}$. The respective reaction rate constant in methanol is 2.7×10^{-5} s^{-1} ($C_{Ir} = 3.3 \times 10^{-4}$ mol L^{-1}, 299 K).[18] In ethanol−isopropanol mixtures, the solvent-induced reduction of $[IrCl_6]^{2-}$ does not involve the coordination sphere of the central metal ion.[19]

In this paper, we report on some peculiarities of the reaction between $H_2IrCl_6{\cdot}6H_2O$ and $Na_2[IrCl_6]{\cdot}nH_2O$ with DMSO and acetone. In particular, we elaborate a preparative protocol for $[H(dmso)_2][IrCl_5(dmso\text{-}\kappa O)]$ and accomplish spectroscopic and structural characterization of the latter compound. Furthermore, we isolate and characterize byproducts of the reaction, viz., $[H(dmso)_2][trans\text{-}IrCl_4(dmso\text{-}\kappa S)_2]$ and $[H(dmso)][trans\text{-}IrCl_4(dmso\text{-}\kappa S)_2]$.

RESULTS AND DISCUSSION

Behavior of $[IrCl_6]^{2-}$ in DMSO Solutions. Aiming at the preparation of iridium(IV) dimethyl sulfoxide complexes, we elucidated the reactivity of $[IrCl_6]^{2-}$ in the forms of sodium hexachloridoiridate or hexachloridoiridic acid toward DMSO. As a monitor, we utilized spectrophotometry since $[IrCl_6]^{2-}$ ions manifest very intense ligand-to-metal charge transfer signals in UV−Vis absorption spectra, which are highly sensitive to minute changes in the coordination sphere of the iridium atoms.[20]

The long-term storage of $Na_2[IrCl_6]{\cdot}nH_2O$ solutions in DMSO was found to be accompanied by a very slow attenuation of original absorption bands assigned to the $[IrCl_6]^{2-}$ ions (Figure 1), which assumes that the reduction of iridium(IV) to iridium(III) takes place. It is known that d−d transitions observed in the visible spectral range for iridium(III)-derived chloride complexes are weaker than those typical of $[IrCl_6]^{2-}$ by more than one order of magnitude, and thus, they are extremely difficult to be detected in the presence of residual iridium(IV) species.[13,15,21−24]

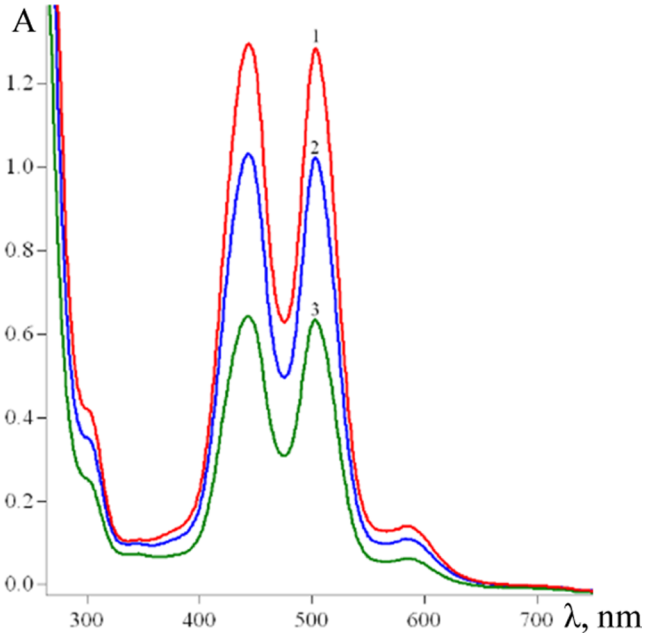

Figure 1. Time evolution of UV−Vis spectra of $Na_2[IrCl_6]{\cdot}nH_2O$ solution in DMSO. $C_{Ir} = 2.5 \times 10^{-3}$ mol·L^{-1}; τ = 3 min (1, red); 200 days (2, blue); 2.5 years (3, green).

Meanwhile, the exact shape of absorption bands remains unchanged, which means that the residual iridium(IV) was still in the chemical form of $[IrCl_6]^{2-}$. The apparent changes in the intensity of bands peaked at 444 and 503 nm can be used to evaluate the degree of conversion of iridium(IV) into iridium(III). The reduction degree is independent of the wavelength chosen for the evaluation. Furthermore, the apparent reduction degree gets increased for dilute solutions (Figure 2).

In mixed solvent systems, such as DMSO−acetone or DMSO−ethanol, the reduction proceeds much faster (Figure 2).

Solutions of $H_2IrCl_6{\cdot}6H_2O$ in DMSO behave similarly. The character of the process is not altered upon heating (to either 90 or 150 °C) although the apparent reduction rate increases prominently (Figure 3). More specifically, the half-conversion time of $H_2[IrCl_6]$ is 2 h at 150 °C ($C_{Ir} = 3.0 \times 10^{-3}$ mol·L^{-1}).

The above results concern UV−Vis monitoring. The time evolution of EPR spectra of $H_2IrCl_6{\cdot}6H_2O$ solutions in DMSO after heating at 150 °C are shown in Figure 4. Similar to the UV−Vis spectra, a decrease in the EPR signal amplitude and its integral intensity is observed. This undoubtedly means that the initial Ir(IV) ions are reduced to nonparamagnetic Ir(III) species without important changes in the coordination sphere of Ir(IV) ions. The latter conclusion follows from the observation that all experimental EPR spectra are characterized by identical shapes until at least 6.5 h of reaction duration.

Computer simulation of the experimental spectral singlets (compare solid and open circle lines in Figure 4, curve a) allowed us to determine the EPR parameters. They are g_0 = 1.780 ± 0.003 and the peak-to-peak linewidth ΔB = 26 ± 0.5 mT.

Based on the results discussed above, we can conclude that no formation of iridium(IV) dimethyl sulfoxide coordination compounds occurs at the iridium concentrations explored, or the reaction extent is below detection limits of the instrumental techniques applied.

Behavior of $[IrCl_6]^{2-}$ in Acetone Solutions. Among methods used for the preparation of PM(IV) dimethyl sulfoxide coordination compounds, we would like to mention a trick of using intermediate labile complexes of Ir(IV) with solvent molecules as ligands. In particular, such a trick worked well for the case of osmium and acetone[25]

$$[MCl_6]^{2-} \rightarrow [MCl_5(Me_2CO)]^{-} \rightarrow [MCl_5(dmso)]^{-}$$

In order to test this approach in the case of Ir(IV), we explored the behavior of $[IrCl_6]^{2-}$ upon long-term storage in acetone.

UV−Vis spectra of $Na_2[IrCl_6]{\cdot}nH_2O$ solutions in acetone ($C_{Ir} = n \times 10^{-3}$ mol·L^{-1}) evolve in time in a way similar to DMSO solutions. We observe no signature of formation of Ir(IV)-based complexes with acetone molecules as ligands. At $C_{Ir} = 3 \times 10^{-3}$ mol·L^{-1}, the half-conversion time of $[IrCl_6]^{2-}$ is about 3 months. The apparent reduction rate is significantly decreased for more dilute solutions. Indeed, the UV−Vis spectra remain essentially unchanged for 6 months of aging at an iridium concentration of $C_{Ir} = 3 \times 10^{-4}$ mol·L^{-1}.

https://doi.org/10.1021/acsomega.3c01012
ACS Omega 2023, 8, 20569−20578

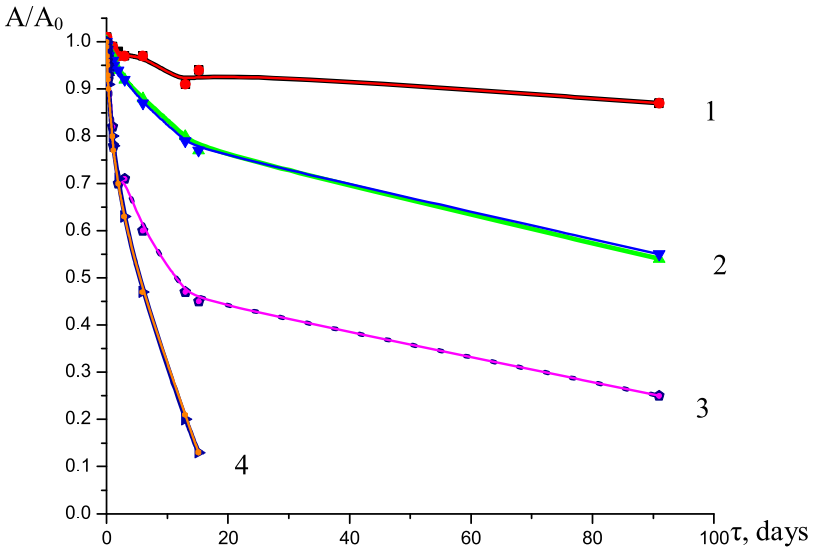

Figure 2. Apparent attenuation (A/A_0) of the UV−Vis absorption bands as a function of time for $Na_2[IrCl_6]\cdot nH_2O$ solutions in DMSO (curves 1,2) and in mixed solvent systems DMSO + acetone (90 vol % of acetone) (curve 3), and DMSO + ethanol (90 vol % of ethanol) (curve 4). C_{Ir} = 2.5 × 10^{-3} mol·L^{-1} (1), 2.5 × 10^{-4} mol·L^{-1} (2−4); λ = 444, 503 nm (1, 2); 440, 495 nm (3, 4).

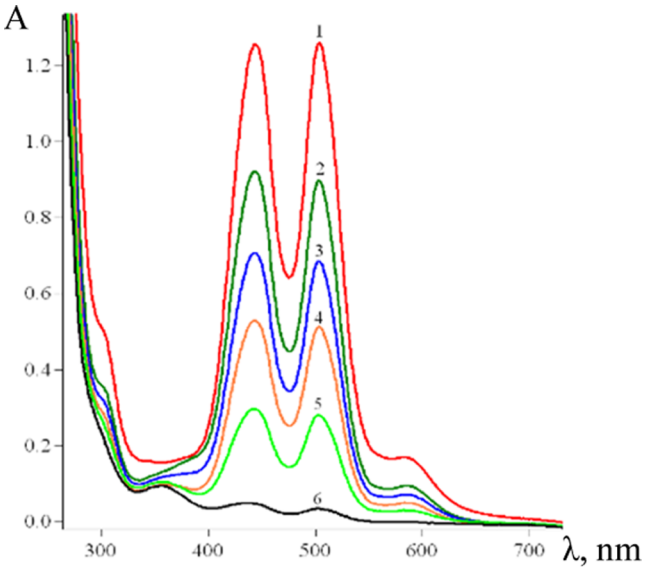

Figure 3. Time evolution of UV−Vis spectra of $H_2IrCl_6\cdot 6H_2O$ solutions in DMSO. C_{Ir} = 3.0 × 10^{-3} mol·L^{-1}; starting solution (1); solution aged for 1 h (2), 2 h (3), 3.5 h (4), 6.5 h (5), and 8.5 h (6) at 150 °C.

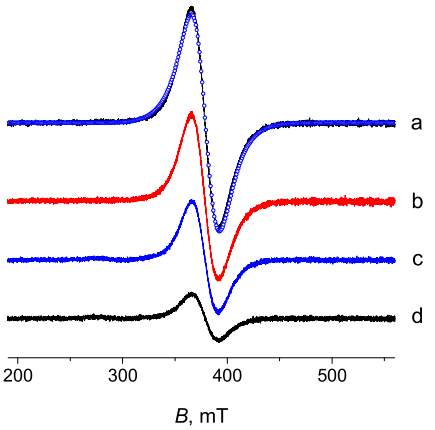

Figure 4. Experimental (solid lines) and simulated (open circles) EPR spectra of $H_2IrCl_6\cdot 6H_2O$ solutions in DMSO: initial (a) and after 2 h (b), 3.5 h (c), and 6.5 h (d) of the reaction at 150 °C (the EPR spectra were recorded at 90 K).

Ultimately, the long-term aging of $Na_2[IrCl_6]\cdot nH_2O$ in acetone solutions afforded a precipitate. We isolated this precipitate and applied single-crystal X-ray diffraction to establish its chemical identity as $Na_3[IrCl_6]\cdot 2H_2O$. Since no crystal structure of such a salt has been reported so far, we describe the respective crystallographic results below.

Importantly, the UV−Vis spectra of acetone solutions of another precursor, $H_2IrCl_6\cdot 6H_2O$, evolve differently with respect to $Na_2[IrCl_6]\cdot nH_2O$ solutions. The process can be formally divided into several stages. At the first stage, the absorption bands peaked at 460 and 550 nm slightly increase in intensity at the costs of correlated attenuation of absorption bands at 420 and 491 nm ascribed to pristine $[IrCl_6]^{2-}$ anions (Figure 5a).

At this stage, the series of spectra pass through a few isosbestic points, which typically assumes that the system is composed of two absorbing components. Most probably, the interaction product should remain in the Ir(IV) oxidation state since the overall variations of the signal intensity are insignificant. The second component present in the solutions in addition to pristine $[IrCl_6]^{2-}$ is characterized by UV−Vis peaks at 460 nm and shoulders at 353, 420, 495, and 556 nm (Figure S1 of Supplementary Materials).

It is known that the Ir(IV) pentachloride monoaqua complex $[IrCl_5(H_2O)]^-$ is characterized by an absorption band at λ_{max} = 450 nm (ε = 3320 $mol^{-1}\cdot L\cdot cm^{-1}$).[13] The UV−Vis maximum of $[IrCl_5(MeOH)]^-$ in methanol is observed at 450 nm.[18] A similar spectrum is also expected for the monoacetone pentachloride complex with an acetone ligand coordinated to the Ir site via the oxygen atom. Thus, we assume that it is $[IrCl_5(Me_2CO)]^-$ that is formed spontaneously upon prolonged storage of H_2IrCl_6 in acetone.

The apparent rate of the monoacetone complex formation increases with an increase in $H_2IrCl_6\cdot 6H_2O$ concentration

https://doi.org/10.1021/acsomega.3c01012
ACS Omega 2023, 8, 20569−20578

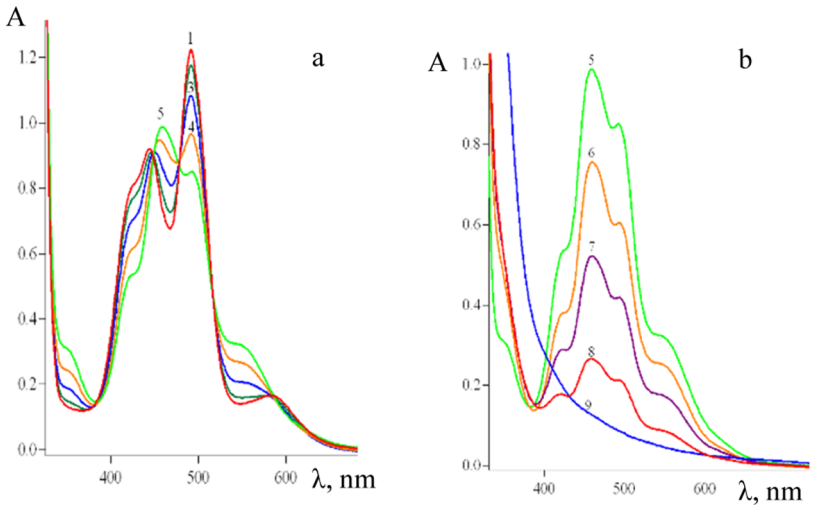

Figure 5. Time evolution of UV−Vis spectra of $H_2IrCl_6{\cdot}6H_2O$ solutions in acetone. $C_{Ir} = 2.8 \times 10^{-4}$ mol·L^{-1}; $l = 1.0$ cm. (a) $\tau = 2$ min (1), 4 h (2), 23 h (3), 2 days (4), 5 days (5); (b) $\tau = 5$ days (5), 26 days (6), 34 days (7), 37 days (8), 166 days (9).

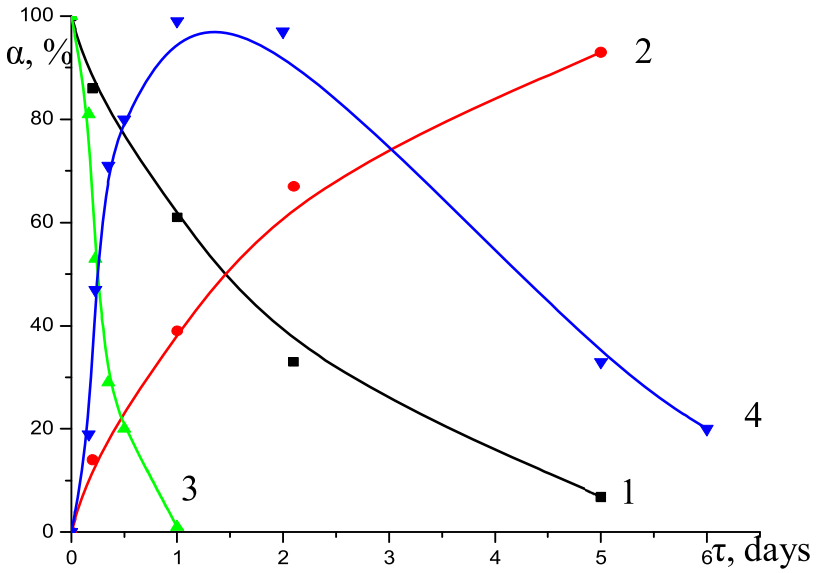

Figure 6. Composition of dominant species for $H_2IrCl_6{\cdot}6H_2O$ solutions in acetone at room temperature as a function of time: $C_{Ir} = 2.8 \times 10^{-4}$ mol·L^{-1} (curves 1 and 2), $C_{Ir} = 3.5 \times 10^{-3}$ mol·L^{-1} (curves 3 and 4). The graphs show molar fractions of $[IrCl_6]^{2-}$ (curves 1 and 3) and molar fractions of $[IrCl_5(Me_2CO)]^-$ (curves 2 and 4).

(Figure 6). Indeed, the half-conversion times are 35 h and 6 h for $H_2IrCl_6{\cdot}6H_2O$ concentrations of 2.8×10^{-4} and 3.5×10^{-3} mol·L^{-1}, respectively.

An increase in temperature accelerates the reaction significantly. The formation of the monoacetone complex at 3×10^{-3} mol·L^{-1} takes as short as 20 min at 46 °C.

The EPR spectroscopy study of $H_2IrCl_6{\cdot}6H_2O$ solutions in acetone (6×10^{-3} mol·L^{-1}) also supports the formation of a novel iridium(IV) complex under these conditions.

Typical changes occurring with the EPR spectra during the first 20 min of the reaction at an elevated temperature are shown in Figure 7. We interpret the changes observed as a rearrangement in the coordination sphere of the iridium ion, i.e., $[IrCl_6]^{2-} \rightarrow [IrCl_5(Me_2CO)]^-$ conversion. Indeed, a single isotropic line is typical of the initial high-symmetry $[IrCl_6]^{2-}$, while a doublet line with anisotropic $g_{\parallel}$ and $g_{\perp}$ components may well correspond to an asymmetric $[IrCl_5(Me_2CO)]^-$ moiety. Note that during the first 20 min of reaction duration, the total concentrations of both paramagnetic centers stay constant within the instrumental error limit.

After a certain induction period, the total intensity of UV−Vis spectra starts to decrease due to the reduction of iridium(IV). However, this decrease is not accompanied by any significant changes in relative intensities of bands at 460 and 490 nm (Figure 5b). The reduction reaction proceeds at a lower rate than the ligand exchange (Figures 5b and 6); the respective half-conversion time for the monoacetone complex at a concentration of 2.8×10^{-4} mol L^{-1} is about 25 days. The apparent reduction rate is increased for more concentrated solutions. Indeed, the half-conversion time for the monoacetone complex at a concentration of $n \times 10^{-3}$ mol·L^{-1} is 2−3 days.

Synthesis and Characterization of [H(dmso)$_2$][IrCl$_5$(dmso-κO)] (1). The aged solution of $H_2IrCl_6{\cdot}6H_2O$ in acetone, in which the conversion into $[IrCl_5(Me_2CO)]^-$ was complete according to UV−Vis spectroscopy, was successfully used to

https://doi.org/10.1021/acsomega.3c01012
ACS Omega 2023, 8, 20569−20578

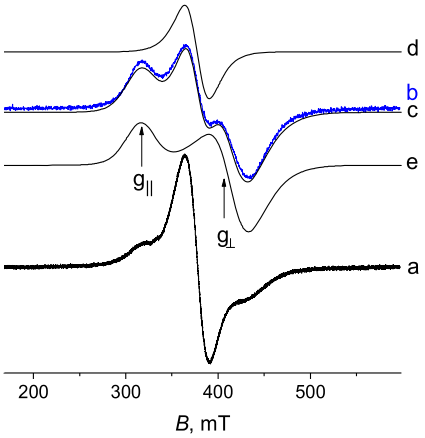

Figure 7. Experimental (a, b) and simulated (c–e) EPR spectra of $H_2IrCl_6{\cdot}6H_2O$ solutions in acetone (at 90 K) after 6 h of aging at room temperature (a) and after 15 min of aging at 40 °C (b). The spectrum (c) is the sum of a singlet (d) and a doublet (e).

prepare a novel Ir(IV) complex $[H(dmso)_2][IrCl_5(dmso\text{-}\kappa O)]$ (**1**). There are two ways to achieve the full conversion of H_2IrCl_6 into $[IrCl_5(Me_2CO)]^-$: (a) aging at room temperature for ∼24 h and (b) aging at an elevated temperature of 40–50 °C for ∼20 min. The addition of DMSO to such an aged solution results in immediate precipitation of red crystals.

Despite the quantitative conversion of iridium species into the monoacetone form, the addition of DMSO to these acetone solutions first gives rise to the precipitation of small amounts of $[H(dmso)_2]_2[IrCl_6]$ as red crystals, but then the major fraction precipitates as $[H(dmso)_2][IrCl_5(dmso\text{-}\kappa O)]$.

The preparation of chemically pure $[H(dmso)_2][IrCl_5(dmso\text{-}\kappa O)]$ is a challenge since the reaction typically yields a mixture of complexes. If solutions with the only partial conversion of iridium species into the monoacetone form are used as a reactant for the reaction with DMSO, then red crystals of $[H(dmso)_2]_2[IrCl_6]$ coprecipitate along with **1**. If the iridium reduction has started, yellow crystals of Ir(III) complexes coprecipitate along with **1**.

The typical occurrence of byproduct companions of **1** in precipitates can be easily confirmed either by a visual inspection of the crystals under an optical microscope or using spectroscopic techniques. EPR spectra of redissolved crystals of the reaction products reveal signals of $[IrCl_6]^{2-}$ ions (Figure S2, Supporting Materials), whereas diamagnetic iridium(III) complexes clearly show up in ^1H NMR spectra.

We have successfully solved crystal structures of two Ir(III) complexes that coprecipitate with **1**, viz., $[H(dmso)_2][trans\text{-}IrCl_4(dmso\text{-}\kappa S)_2]$ (**2**) and $[H(dmso)][trans\text{-}IrCl_4(dmso\text{-}\kappa S)_2]$ (**3**). The former complex is afforded when DMSO is added in high excess.

The separation of the mixtures formed as the reaction products aimed at isolation of **1** can be performed based on their different solubilities in acetone. More specifically, **1** is highly soluble in acetone, $[H(dmso)_2]_2[IrCl_6]$ is characterized by moderate solubility, and iridium(III) complexes are nearly insoluble. The purification of $[H(dmso)_2][IrCl_5(dmso\text{-}\kappa O)]$ from admixtures of Ir(III) complexes can be realized via the extraction with acetone followed by solvent evaporation.

ATR IR spectra of **1** reveal vibrational bands of ν(S═O) groups of the O-coordinated DMSO at 885 cm^{-1} and ν(Ir–O) bands at 501 cm^{-1} along with a broad absorption band spanning over a 550–850 cm^{-1} range and peaked at 717 cm^{-1} typical of ν(S═O—H···O═S) stretching vibration within the monoprotonated DMSO dimer (Figure S3, Supporting Materials). The experimental IR spectrum of **1** is very similar to that of the recently reported analogous osmium complex.[25]

Solid-state UV–Vis spectra of **1** manifest absorption bands at 480 and 560 nm, which differ from those of $[H(dmso)_2]_2[IrCl_6]$ (Figure S4, Supporting Materials).

The ^1H NMR spectrum of **1** in D_2O reveals a singlet signal of methyl protons of pristine DMSO at 2.65 ppm due to the dissociation of $[H(dmso)_2]^+$ cations. The compound **1** is unstable in solutions and a new signal at 3.44 ppm emerges in the spectra, which is typical of DMSO coordinated to Ir(III) via the sulfur atoms.

Crystal Structure of $[H(dmso)_2][IrCl_5(dmso\text{-}\kappa O)]$ (1). According to single-crystal X-ray diffraction study, **1** can be represented as a salt containing $[H(dmso)_2]^+$ cations and $[IrCl_5(dmso\text{-}\kappa O)]^-$ anions. It crystallizes in the orthorhombic syngony, space group $Pca2_1$ with six symmetrically independent formula units per unit cell (Figure 8).

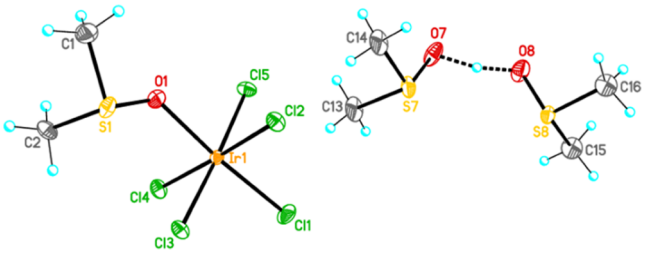

Figure 8. Structure of $[H(dmso)_2][IrCl_5(dmso\text{-}\kappa O)]$ salt (only one out of six independent formula units is shown).

The $[IrCl_5(dmso\text{-}\kappa O)]^-$ anions are conformationally labile with respect to mutual disposition of the DMSO fragment and equatorial chloride ligands. More specifically, four out of six anions adopt the eclipsed confirmation (the respective S═O–Ir–Cl torsion angles are 0.7(11)–9.1(11)°), whereas the other two anions adopt the staggered conformation (the respective S═O–Ir–Cl torsion angles are 37.7(12) and 38.6(11)°).

The DMSO ligands in the $[IrCl_5(dmso\text{-}\kappa O)]^-$ anions are coordinated to the iridium atoms via the oxygen atoms, and thus, the coordination environment of Ir is a somewhat distorted octahedron. Due to the *trans*-effect, the Ir–Cl bond lengths for chloride ligands in the *trans*-position with respect to coordinated DMSO are shorter (2.274(7)–2.295(6) Å, $d_{av.}$ = 2.286(7) Å) than the respective bond lengths forming the equatorial plane of the anion (2.274(9)–2.360(9) Å, $d_{av.}$ = 2.321(7) Å). The Ir–O bond length is 2.00(2)–2.118(17) Å. As expected, the S═O bond length in the DMSO fragment coordinated to Ir is longer (1.538(17)–1.57(2) Å) than in the case of free DMSO (1.49 Å).[3,4]

In dimeric cations, the DMSO molecules and H^+ protons are linked by strong O···H···O hydrogen bonds (the O···O distances are 2.39(3)–2.46(2) Å). They are capable of adopting different conformations determined by mutual dispositions of the DMSO moieties. It is important that all six cations in **1** are characterized by the *cis*-conformation (the S═O···H···O═S torsion angles are 0.1(15)–15.5(16)°).

In the crystal structure, the cations and anions are located at van der Waals distances.

https://doi.org/10.1021/acsomega.3c01012
ACS Omega 2023, 8, 20569–20578

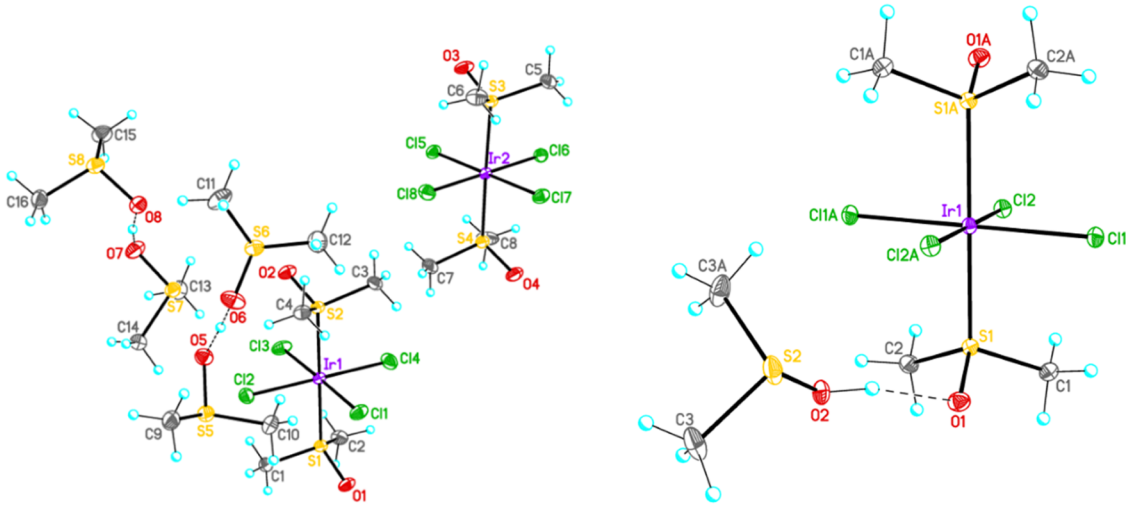

Figure 9. Structures of $[H(dmso)_2][trans\text{-}IrCl_4(dmso\text{-}\kappa S)_2]$ (**2**) (left panel; both symmetrically independent formula units are shown) and $[H(dmso)][trans\text{-}IrCl_4(dmso\text{-}\kappa S)_2]$ (**3**) (right panel).

Table 1. Selected Bond Lengths in $[trans\text{-}Ir^{III}Cl_4(dmso\text{-}\kappa S)_2]^-$, Å[a]

compound	$d(Ir-Cl)_{av}$	$d(Ir-S)_{av}$	$d(S-O)_{av}$	ref
$[H(dmso)][IrCl_4(dmso)_2]$	2.3608(9)	2.3030(12)	1.476(3)	this work
$[H(dmso)][IrCl_4(dmso)_2]$	2.361(4)	2.304(4)	1.476(3)	29
$[H(dmso)_2][IrCl_4(dmso)_2]$	2.3580(10)	2.3100(10)	1.475(3)	this work
$[H(dmso)_2][IrCl_4(dmso)_2]$	2.344(2)	2.327(1)	1.469(4)	6
$[H(dmso)_2][IrCl_4(dmso)_2]$	2.399(7)	2.310(6)		7
$BuNH_3[IrCl_4(dmso)_2]\cdot 0.5H_2O$	2.3576(17)	2.3081(17)	1.472(5)	9
$K[IrCl_4(dmso)_2]\cdot H_2O$	2.3564(12)	2.3112(11)	1.470(3)	9
$K[IrCl_4(dmso)_2]\cdot 0.25H_2O$	2.362(2)	2.309(2)	1.467(7)	9
[H-(nicotine)][$IrCl_4(dmso)_2$]	2.360(3)	2.320(3)	1.459(8)	8
$[Ph_3P(CH_2C(O)CH_3)][IrCl_4(dmso)_2]$	2.3531(8)	2.3199(7)	1.466(2)	30
$[Ph_3P(CH_2CN)][IrCl_4(dmso)_2]$	2.3603(12)	2.3112(12)	1.468(4)	30
$[Ph_3P(CH_2CH{=}CHCH_3)][IrCl(dmso)]$	2.3539(12)	2.3086(15)	1.460(5)	30
$[(Me)_2SCH_2C(O)Me][IrCl_4(dmso)_2]$	2.3576(6)	2.3126(6)	1.474(2)	29

[a]Compounds **2** and **3** differ from each other by the cation type.

Complex **1** is thus the very first structurally characterized example of iridium(IV) halide−dimethyl sulfoxide complex. Closely related compounds are known for platinum and osmium.[25−28] In the osmium complex, the DMSO ligand is coordinated to the central metal ion via the oxygen atom, i.e., exactly in the same way as in **1**. Furthermore, **1** and $[H(dmso)_2][OsCl_5(dmso\text{-}\kappa O)]$ are isostructural.[25] In the platinum complex, the DMSO ligand is coordinated to the platinum site via the sulfur atoms.

*Crystal Structures of $[H(dmso)_2][IrCl_4(dmso\text{-}\kappa S)_2]$ (**2**) and $[H(dmso)][IrCl_4(dmso\text{-}\kappa S)_2]$ (**3**).* Yellow crystals of $[H(dmso)_2][trans\text{-}IrCl_4(dmso\text{-}\kappa S)_2]$ (**2**) and $[H(dmso)][trans\text{-}IrCl_4(dmso\text{-}\kappa S)_2]$ (**3**) were obtained as byproducts during the synthesis of **1**. Their structures were determined by single-crystal X-ray diffraction.

Complex **2** crystallizes in the triclinic syngony, space group *P*-1 with two symmetrically independent formula units per unit cell. It represents a new previously unreported polymorph modification. Previously, a monoclinic modification of $[H(dmso)_2][trans\text{-}IrCl_4(dmso\text{-}\kappa S)_2]$ has been reported, space group $P2/c$[6]/$P2/n$.[7]

The crystal structures of **2** and **3** contain a common $[IrCl_4(dmso\text{-}\kappa S)_2]^-$ anion that adopts the *trans*-configuration. The DMSO ligands are coordinated to the iridium via the sulfur atoms. The S═O groups are characterized by the *trans*-configurations (Figure 9).

The Ir−Cl, Ir−S, and S═O bond lengths in these anions correspond well to respective values reported for other compounds with the $[trans\text{-}IrCl_4(dmso\text{-}\kappa S)_2]^-$ anions (Table 1). The S═O bond lengths in the anions (Table 1) are shortened with respect to those typical of uncoordinated DMSO (1.49 Å).[3,4]

The $[trans\text{-}IrCl_4(dmso\text{-}\kappa S)_2]^-$ configuration is the most typical form of Ir(III) chloride−dimethyl sulfoxide complexes. The vast majority of structural reports reveal this moiety in iridium-based coordination compounds with DMSO as a ligand (Table 1). Similar $[trans\text{-}M^{III}Cl_4(dmso\text{-}\kappa S)_2]^-$ anions are encountered in complexes of other PMs, e.g., Rh(III), Ru(III), and Os(III).

The crystal structure of **2** contains dimeric monoprotonated cations $[H(dmso)_2]^+$ (Figure 9) with strong O···H···O hydrogen bonds (the O···O distances are 2.427(4) and 2.438(4) Å), which are quite typical of DMSO crystal chemistry. These moieties adopt the *trans-gauche-* and *trans*-conformations (the respective S═O···H···O═S torsion angles are 154.7(3) and 177.7(2)°).

Complex **3** crystallizes in the orthorhombic syngony, space group *Pccn*. In the crystal structure of **3**, a rather rare

https://doi.org/10.1021/acsomega.3c01012
ACS Omega 2023, 8, 20569−20578

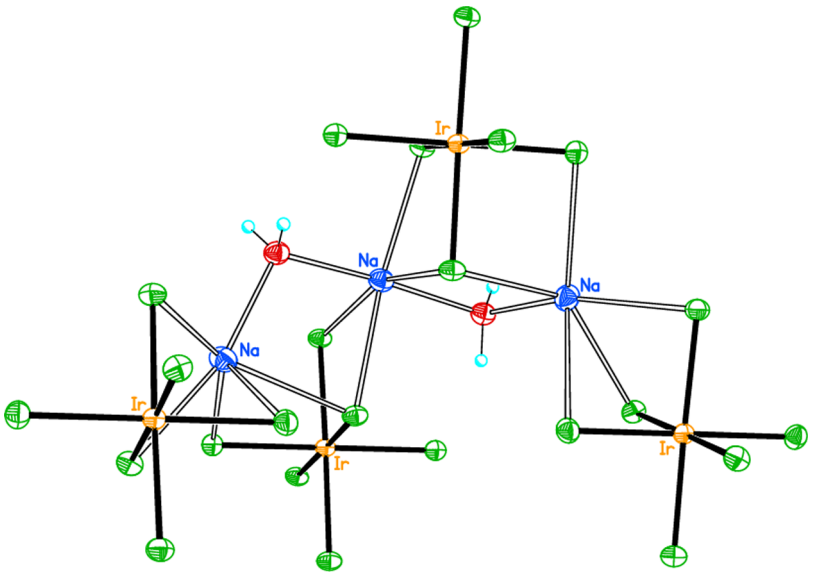

Figure 10. Fragment of the crystal structure of $Na_3[IrCl_6]\cdot 2H_2O$ (the $[IrCl_6]$ octahedra occupy special positions on the fourfold axis).

monomeric form of protonated DMSO $[H(dmso)]^+$ acts as the cationic part of the salt. In this cation, the DMSO fragment is protonated at the oxygen atom. The hydrogen atom of the OH group in the cation forms a hydrogen bond with the oxygen atom of the DMSO ligand in the anion (Figure 9). Recently, we have reported the crystal structure of the compound $[H(dmso)][Ir^{III}Cl_4(dmso\text{-}\kappa S)_2]$ corresponding to the space group *Ama*2. In that structure, the hydrogen atom of the OH group forms a hydrogen bond with Cl ligands of the anion.[29] Thus, we describe herewith a novel polymorph modification of $[H(dmso)][trans\text{-}Ir^{III}Cl_4(dmso\text{-}\kappa S)_2]$.

There are a few compounds of other platinum metals containing the $[H(dmso)]^+$ cation,[31−34] in particular, $[H(dmso)][trans\text{-}Ru^{III}Cl_4(dmso\text{-}\kappa S)_2]$.[32] The ruthenium compound is isostructural to **3**.

Analogous polymorphs were reported by Gamage et al.[35] for $(Et_2NH_2)[trans\text{-}Rh^{III}Cl_4(dmso\text{-}\kappa S)_2]$ with cations forming H-bonds with either Cl atoms or oxygen atoms of the DMSO ligand. The authors introduced a special term "H-bond acceptor structural isomers" to emphasize these unique crystal design factors.

Crystal Structure of $Na_3[IrCl_6]\cdot 2H_2O$ (4). Compound **4** was afforded by aging of the $Na_2[IrCl_6]\cdot nH_2O$ solution in acetone. In the anionic part, the $[IrCl_6]^{3-}$ fragments are characterized by the octahedral coordination (Figure 10), the mean Ir—Cl bond length is 2.3568(11) Å, and this value should be compared with the respective value of 2.31 Å in a related Ir(IV) complex $Na_2[IrCl_6]\cdot 2H_2O$.[36]

Among known hexachloridoiridates(III), the Ir−Cl bond lengths are 2.352(5)−2.373(4) and 2.341(2)−2.380(2) Å in $K_3[IrCl_6]$[37,38] and $(NH_4)_2[IrCl_6]\cdot H_2O$,[37] respectively. The coordination environment of sodium atoms is formed by five chloride ligands and one oxygen atom of the hydrate water molecule in the configuration of a distorted octahedron.

CONCLUSIONS

The reaction of $H_2IrCl_6\cdot 6H_2O$ or $Na_2[IrCl_6]\cdot nH_2O$ with DMSO results in a slow reduction of Ir(IV) avoiding the formation of Ir(IV) dimethyl sulfoxide complexes in measurable quantities. But the reaction of $H_2IrCl_6\cdot 6H_2O$ with acetone results in $[IrCl_5(Me_2CO)]^-$ at the first stage. The aged solution of $H_2IrCl_6\cdot 6H_2O$ in acetone, in which the conversion into $[IrCl_5(Me_2CO)]^-$ was complete, was successfully used to prepare a novel Ir(IV) complex $[H(dmso)_2][IrCl_5(dmso\text{-}\kappa O)]$. New polymorph modifications of known iridium(III) complexes $[H(dmso)_2][trans\text{-}IrCl_4(dmso\text{-}\kappa S)_2]$ and $[H(dmso)][trans\text{-}IrCl_4(dmso\text{-}\kappa S)_2]$ were isolated and structurally elucidated as byproducts of the above reaction.

EXPERIMENTAL SECTION

$H_2IrCl_6\cdot 6H_2O$ (40% Ir) and $Na_2[IrCl_6]\cdot 6H_2O$ reactants were purchased from Acros Organics. It is known[36] that the amount of hydration water in the latter salt is variable being the function of ambient humidity. In the present synthesis, the reactant contained two hydration water molecules per formula unit.

Synthesis of $[H(dmso)_2][IrCl_5(dmso\text{-}\kappa O)]$ (1). A. A load of 0.10 g of $H_2IrCl_6\cdot 6H_2O$ was dissolved in 50 mL of acetone and aged for ∼24 h until complete conversion into $[IrCl_5(Me_2CO)]^-$ (as controlled by UV−Vis). Then, 0.30 ml of DMSO was added to the aged solution and then 75 mL of diethyl ether. A small amount of dark red precipitate formed was filtered off and identified as $[H(dmso)_2]_2[IrCl_6]$ (using UV−Vis and IR). The dominant fraction of the precipitate formed in one day. The precipitate was filtered off. Under inspection with an optical microscope, the polycrystalline powder was a mixture of red plate-shaped and yellow needle-shaped crystals. The mixture was treated with acetone to dissolve red crystals and keep yellow crystals intact. The precipitation of oily product afforded after acetone evaporation was induced by adding ∼2 mL of diethyl ether. The fine red crystalline precipitate was filtered off. Mass of the product was 0.043 g (37% yield with respect to Ir).

B. A load of 0.14 g of $H_2IrCl_6\cdot 6H_2O$ was dissolved in 75 ml of acetone. The solution was heated to 50 °C and aged for 20 min until complete conversion into $[IrCl_5(Me_2CO)]^-$ (as controlled by UV−Vis) and 0.30 mL of DMSO was added to the mixture. A small amount of dark red precipitate formed immediately was filtered off and identified as $[H(dmso)_2]_2[IrCl_6]$ (using UV−Vis and IR). To the remaining reaction mixture, 30 ml of diethyl ether was added. The dominant fraction of the precipitate formed in one day. The

https://doi.org/10.1021/acsomega.3c01012
ACS Omega 2023, 8, 20569−20578

Table 2. Crystallographic and Structure Refinement Parameters of $[H(dmso)_2][IrCl_5(dmso\text{-}\kappa O)]$ (1), $[H(dmso)_2][trans\text{-}IrCl_4(dmso\text{-}\kappa S)_2]$ (2), $[H(dmso)][trans\text{-}IrCl_4(dmso\text{-}\kappa S)_2]$ (3), and $Na_3[IrCl_6]\cdot 2H_2O$ (4)

compound	1	2	3	4
empirical formula	$C_6H_{19}Cl_5IrO_3S_3$	$C_8H_{25}Cl_4IrO_4S_4$	$C_6H_{19}Cl_4IrO_3S_3$	$Cl_6H_4IrNa_3O_2$
formula weight	604.86	647.54	569.41	509.92
crystal size, mm^3	0.03 × 0.02 × 0.01	0.15 × 0.08 × 0.08	0.12 × 0.10 × 0.09	0.20 × 0.10 × 0.10
wavelength, Å	0.74500	0.74500	0.74500	0.71073
crystal system	orthorhombic	triclinic	orthorhombic	tetragonal
space group	$Pca2_1$	*P*-1	*Pccn*	*P*4/*ncc*
a, Å	24.293(2)	9.1060(13)	9.0390(16)	10.5638(3)
b, Å	22.848(2)	13.8940(16)	13.440(2)	10.5638(3)
c, Å	19.8370(17)	16.419(2)	13.619(2)	20.1299(6)
α, °	90	90.834(12)	90	90
β, °	90	90.540(11)	90	90
γ, °	90	100.687(14)	90	90
V, $Å^3$	11 010.5(16)	2040.9(5)	1654.5(5)	2246.37(14)
Z	24	4	4	8
d, g/cm^3	2.189	2.108	2.286	3.016
μ, mm^{-1}	9.387	8.421	10.226	13.385
F(000)	6936	1256	1088	1856
θ_{max}, °	26.00	31.08	31.12	32.61
reflections collected	68 416	44 304	16 946	24 931
independent reflections, R_{int}	18 651, 0.0709	11 014, 0.0356	2282, 0.0306	2060, 0.0592
reflections observed ($I > 2\sigma(I)$)	13226	10018	1931	1545
R_1 ($I > 2\sigma(I)$)	0.0591	0.0324	0.0295	0.0241
wR_2 (all data)	0.1196	0.0837	0.0805	0.0510
GOOF	1.003	1.024	1.021	1.106
extinction coefficient		0.00165(14)	0.0024(2)	
T_{min}/T_{max}	0.743/0.891	0.308/0.494	0.302/0.385	0.212/0.252
$\Delta\rho_{max}/\Delta\rho_{min}$, $\bar{e}Å^3$	5.323/−2.273	4.231/−2.103	0.996/−1.636	0.983/−1.652

precipitate was filtered off. Under visual inspection with an optical microscope, the polycrystalline product was a mixture of red plate-shaped and yellow needle-shaped crystals. The further treatment was the same as in protocol **A**. Mass of the product was 0.044 g (26% yield with respect to Ir).

The compound is soluble in water, acetone, and DMSO to form red solutions.

UV−Vis (λ_{max}, nm (ε, $mol^{-1}\cdot L\cdot cm^{-1}$)): H_2O $-297_{sh}(900)$, $409_{sh}(1840)$, 454(2390), $554_{sh}(705)$; DMSO $-392_{sh}(1510)$, 446(2690), 470(2740), $550_{sh}(1285)$; polycrystalline powder: −480, 560 nm.

ATR IR (ν, cm^{-1}): 420, 501, 682, 717, 885, 946, 984, 1015, 1320, 1400, 2912, and 3004.

^1H NMR in D_2O 2.65 ppm.

UV−Vis spectra were measured with a VARIAN CARY 50 spectrophotometer. UV−Vis spectra for polycrystalline powders were measured using nujol suspensions spread over two quartz plates.

ATR IR spectra were measured with a Bruker Alpha FT-IR spectrometer equipped with a Platinum ATR unit.

^1H NMR spectra were measured with a Spinsolve 90 Carbon spectrometer at an operation frequency of 90 MHz. D_2O was used as a solvent. The signals were references against those of residual undeuterated water.

EPR spectra were recorded using a Bruker EMX500 Plus X-band spectrometer equipped with a Bruker temperature control system and a Bruker ER 4119 HS high-sensitivity resonator. The spectra in glass tubes were recorded with an inner diameter of 4.5 mm. The microwave power was adjusted so as to avoid saturation of the EPR signals. The corresponding value was 0.5 mW for frozen solutions and powders at 90 K.

Powder X-ray diffraction patterns were measured at the X-ray structural analysis beamline of the Kurchatov Synchrotron Radiation Source (NRC Kurchatov Institute, Moscow, Russia) at λ = 0.74000 Å using a Rayonix SX-165 CCD detector. The sample-to-detector distance was 100 mm, and the exposure time was 10 min.

Single-Crystal X-ray Diffraction Studies. Single crystals appropriate for measurements were fished from bulk polycrystalline mixtures. The measurements for **1**, **2** were carried out at the same X-ray structural analysis beamline of the Kurchatov Synchrotron Radiation Source using a Rayonix SX-165 CCD detector (T = 100 K, λ = 0.74500 Å). In total, 720 frames were collected with an oscillation range of 1.0° in the φ scanning mode using two different orientations for each crystal. The semiempirical correction for absorption was applied using the *Scala* program.[39] The data were indexed and integrated using the utility *iMOSFLM* from the CCP4 software suite.[40,41] The single-crystal X-ray diffraction data for **3**, **4** were collected with a three-circle Bruker D8 QUEST diffractometer (T = 100 K, λ(Mo$K\alpha$)-radiation, graphite monochromator, ω- and φ-scanning mode). The data were indexed and integrated using the *SAINT* program[42] and then scaled and corrected for absorption using the *SADABS* program.[43] For details, see Table 2.

The structures were solved by the intrinsic phasing modification of direct methods[44] and refined by a full-matrix least-squares technique on F^2 with anisotropic displacement parameters for all nonhydrogen atoms. The hydrogen atoms of the OH groups as well as of the water molecule were objectively localized in the difference Fourier maps and included in the refinement within the riding model with

https://doi.org/10.1021/acsomega.3c01012
ACS Omega 2023, 8, 20569−20578

fixed isotropic displacement parameters [U_{iso}(H) = 1.5U_{eq}(O)]. The other hydrogen atoms were placed in calculated positions and refined within the riding model with fixed isotropic displacement parameters [U_{iso}(H) = 1.5U_{eq}(C) for the CH_3 groups and 1.2U_{eq}(C) for the other groups]. All calculations were carried out using the *SHELXTL* program.[45,46]

The experimental X-ray powder diffraction pattern of **1** was essentially identical to the one simulated theoretically from crystallographic data for [H(dmso)$_2$][$IrCl_5$(dmso)] (Figure S4, Supporting Materials), which justified the strict phase purity of the as-synthesized sample.

■ ASSOCIATED CONTENT

Supporting Information

The Supporting Information is available free of charge at https://pubs.acs.org/doi/10.1021/acsomega.3c01012.

Data_1: audit_creation_method (SHELXL-2013)

Data_2: audit_creation_method (SHELXL-2013)

Data_3: audit_creation_method (SHELXL-2013)

Data_4: audit_creation_method (SHELXL-2018/3)

Deconvolution of experimental UV−Vis spectra of $H_2IrCl_6{\cdot}nH_2O$; EPR spectrum; ATR IR spectra; UV−Vis spectra for polycrystalline powders; and powder diffraction pattern (PDF)

■ AUTHOR INFORMATION

Corresponding Authors

Olga V. Rudnitskaya − *Department of Inorganic Chemistry, Peoples' Friendship University of Russia (RUDN University), Moscow 117198, Russian Federation*; Email: orudnitskaya@rambler.ru

Victor N. Khrustalev − *Department of Inorganic Chemistry, Peoples' Friendship University of Russia (RUDN University), Moscow 117198, Russian Federation; Zelinsky Institute of Organic Chemistry RAS, Moscow 119991, Russian Federation*; orcid.org/0000-0001-8806-2975; Email: vnkhrustalev@gmail.com

Authors

Tatiana A. Tereshina − *Department of Inorganic Chemistry, Peoples' Friendship University of Russia (RUDN University), Moscow 117198, Russian Federation*

Ekaterina V. Dobrokhotova − *Department of Inorganic Chemistry, Peoples' Friendship University of Russia (RUDN University), Moscow 117198, Russian Federation*

Ekaterina K. Kultyshkina − *Department of Inorganic Chemistry, Peoples' Friendship University of Russia (RUDN University), Moscow 117198, Russian Federation*

Natalia A. Chumakova − *Semenov Federal Research Center for Chemical Physics RAS, Moscow 119991, Russian Federation; Chemistry Department, Lomonosov Moscow State University, Moscow 119991, Russian Federation*; orcid.org/0000-0002-3058-2254

Alexander I. Kokorin − *Semenov Federal Research Center for Chemical Physics RAS, Moscow 119991, Russian Federation*

Yan V. Zubavichus − *Synchrotron Radiation Facility SKIF, Boreskov Institute of Catalysis SB RAS, Koltsovo 630559, Russian Federation*

Complete contact information is available at: https://pubs.acs.org/10.1021/acsomega.3c01012

Notes

The authors declare no competing financial interest.

■ ACKNOWLEDGMENTS

This study has been supported by the RUDN University Scientific Projects Grant System, project No. 025239-2-000. N. A. Chumakova and A. I. Kokorin are indebted Russian Foundation for Basic Research (Project No 21-53-54001). This work was performed partially within the framework of the Program of Fundamental Research of the Russian Federation (Reg. No 122040500068-0).

■ REFERENCES

(1) Kukushkin, Yu.N. The contribution of studies on dimethyl sulfoxide complexes to theoretical coordination chemistry. *Russ. J. Coord. Chem.* **1997**, *23*, 149−159.

(2) Calligaris, M.; Carugo, O. Structure and bonding in metal sulfoxide complexes. *Coord. Chem. Rev.* **1996**, *153*, 83−154.

(3) Calligaris, M. Stereochemical aspects of sulfoxides and metal sulfoxide complexes. *Croat. Chem. Acta* **1999**, *72*, 147−169.

(4) Alessio, E. Synthesis and Reactivity of Ru-, Os-, Rh-, and Ir-Halide-Sulfoxide Complexes. *Chem. Rev.* **2004**, *104*, 4203−4242.

(5) Haddad, Y. M. Y.; Herbest, H. B.; Trocha-Grimshaw, J. J. Aspects of Catalysis. Part II. Dimethyl Sulphoxide Complexes of Iridium(III) Including Hydrides. *Chem. Soc., Perkin Trans. 1* **1974**, 592−595.

(6) Cartwright, P. S.; Gillard, R. D.; Sillanpaa, E. R. J.; Valkonen, J. [Bis(dimethylsulphoxide)protium][trans-bisdimethylsulphoxidetetrachloroiridate(III)]. *Polyhedron* **1988**, *9* (21), 2143−2148.

(7) Messori, L.; Marcon, G.; Orioli, P.; Fontani, M.; Zanello, P.; Bergamo, A.; Sava, G.; Mura, P. J. Molecular structure, solution chemistry and biological properties of the novel [ImH][trans-IrCl(4)(Im)(DMSO)], (I) and of the orange form of [(DMSO)(2)H][trans-IrCl(4)(DMSO)(2)], (II), complexes. *Inorg. Biochem.* **2003**, *95*, 37−46.

(8) Albertí, F. M.; Fiol, J. J.; Garcia-Raso, A.; Torres, M.; Terron, A.; Barcelo-Oliver, M.; Prieto, M. J.; Moreno, V.; Molins, E. Ruthenium(III) and iridium(III) complexes with nicotine. *Polyhedron* **2010**, *29*, 34−41.

(9) Ridgway, B. M.; Foi, A.; Corrêa, R. S.; Bikiel, D. E.; Ellena, J.; Doctorovich, F.; Di Salvo, F. Conformational and structural diversity of iridium dimethyl sulfoxide complexes. *Acta Crystallogr., Sect. B: Struct. Sci.* **2017**, *73*, 1032−1042.

(10) Lagos, Y.; Palou-Mir, J.; Bauzá, A.; Fiol, J. J.; Garcia-Raso, Á.G.; Terrón, A.; Molins, E.; Barceló-Oliver, M.; Frontera, A. New chloride-dimethylsulfoxide-iridium(III) complex with histaminium. *Polyhedron* **2015**, *102*, 735−740.

(11) Dorta, R.; Rozenberg, H.; Shimon, L. J. W.; Milstein, D. Oxidative Addition of Water to Novel Ir(I) Complexes Stabilized by Dimethyl Sulfoxide Ligands. *J. Am. Chem. Soc.* **2002**, *124*, 188−189.

(12) Blasius, E.; Preetz, W.; Schmitt, R. Untersuchung des verhaltens der chlorokomplexe der platinelemente in Lösung und an anionenaustauschern. *J. lnorg. Nucl. Chem.* **1961**, *19*, 115−132.

(13) Poulsen, I. A.; Garner, C. S. A thermodynamic and kinetic study of hexachloro and aquopentachloro complexes of iridium(III) in aqueous solutions. *J. Am. Chem. Soc.* **1962**, *84*, 2032−2037.

(14) Cabral Peixoto, J. M. Radiochemical processes in iridium complexes. Products from (n,γ) process in sodium chloroiridate and chloroiridite. *J. Inorg. Nucl. Chem.* **1964**, *26*, 1657−1669.

(15) Moggi, L.; Varani, G.; Manfrin, M. F.; Balzani, V. Photochemical reactions of hexachloroiridate(IV) Ion. *Inorg. Chim. Acta* **1970**, *4*, 335−341.

(16) Alekseeva, I. I.; Romanovskaya, L. E.; Kozlov, A. S. Study of the aquatation process of iridium(III), (IV) chlorocomplexes by kinetic method. *Zh. Neorg. Khim.* **1987**, *32*, 2737−2741.

(17) Sánchez, J. M.; Salvado, V.; Havel, J. Speciation of iridium(IV) in hydrochloric acid medium by means of capillary zone electro-

phoresis and spectrophotometry. *J. Chromatogr. A* **1999**, *834*, 329−340.
(18) Glebov, E. M.; Plyusnin, V. F.; Sorokin, N. I.; Grivin, V. P.; Venediktov, A. B.; Lemmetyinen, H. Photochemistry of $IrCl_6^{2-}$ complex in alcohol solutions. *J. Photochem. Photobiol., A.* **1995**, *90*, 31−37.
(19) Wang, X.-M.; Hu, J.-M.; Zhang, J.-Q. IrO_2−SiO_2 binary oxide films: Preparation, physiochemical characterization and their electrochemical properties. *Electrochim. Acta* **2010**, *55*, 4587−4593.
(20) Jörgensen, K.Ch. Electron transfer spectra of hexahalide complexes. *Mol. Phys.* **1959**, *2*, 309−322.
(21) Jörgensen, K.Ch. Complexes of the 4d- and 5d-Groups. I. Crystal Field Spectra of Rhodium(III) and Iridium(III). *Acta Chem.Scand.* **1956**, *10*, 500−517.
(22) Chang, J. C.; Garner, C. S. Kinetics of Aquation of Aquopentachloroiridate(III) and Chloride Anation of Diaquotetrachloroiridate(III) Anions. *Inorg. Chem.* **1965**, *4*, 209−215.
(23) Eidem, P. K.; Maverick, A. W.; Gray, H. B. Production of hydrogen by irradiation of metal complexes in aqueous solutions. *Inorg. Chim. Acta* **1981**, *50*, 59−64.
(24) Sinitsyn, N. M.; Borisov, V. V.; Kravchenko, V. V.; KozlovA, S.; Prokhodtseva, L. I. Synthesis and research of $K_4[Ir_2Cl_{10}]$. *Zh. Neorg. Khim.* **1982**, *27*, 164−172.
(25) Rudnitskaya, O. V.; Dobrokhotova, E. V.; Kultyshkina, E. K.; Tereshina, T. A.; Trigub, A. L.; Zubavichus, Y. V.; Khrustalev, V. N. Osmium(IV) Halide Complexes with Dimethyl Sulfoxide $[H(dmso)_2][OsX_5(dmso\text{-}\kappa O)]$, X=Cl, Br: Synthesis, Structure, and Properties. *ChemistrySelect* **2020**, *5*, 330−334.
(26) Kukushkin, V.Yu.; Belsky, V. K.; Aleksandrova, E. A.; Pan'kova, E.Yu.; Konovalov, V. E.; Yakovlev, V. N.; Moiseev, A. I. Various Paths and Products of Conversion of Complexes cis-$[Pt(DMSO)(amine)Cl_2]$ under the Influence of $PC1_5$. X-Ray Structure Study of Complexes of Tetraethylammonium Pentachloro(pyridine)platinate-(IV), Tetraethylammonium Trichloro(pyridine)- platinate(II), and Tetraethylammonium Pentachloro(dimethyl sulfoxide)platinate(IV). *J. Gen. Chem.* **1991**, *61*, 318−328.
(27) Sharutin, V. V.; Senchurin, V. S.; Sharutina, O. K.; Gushchin, A. V. Synthesis and structure of platinum complexes $[Ph_4P]^+[PtCl_3(DMSO)]^-$ and $[Ph_4P]^+[PtCl_5(DMSO)]^-$. *Russ. J. Inorg.Chem.* **2013**, *58*, 33−37.
(28) Sharutin, V. V.; Senchurin, V. S.; Sharutina, O. K. Synthesis and structure of the platinum complex $[PH_4Sb(DMSO)][PtCl_5(DMSO)]$. *Butlerov Commun.* **2011**, *28*, 35−39.
(29) Rudnitskaya, O. V.; Tereshina, T. A.; Dobrokhotova, E. V.; Kultyshkina, E. K.; Yakushev, I. A.; Chumakova, N. A.; Kokorin, A. I.; Zubavichus, Y. V.; Khrustalev, V. N. Chemical Evolution in Solutions of Ir Complex $[H(dmso)_2]_2[IrCl_6]$. Structures of $[H(dmso)_2]_2[IrCl_6]$, $[H(dmso)][IrCl_4(dmso)_2]$, $[Me_2SCH_2C(O)Me][IrCl_4(dmso)_2]$, $[Me_2SCH_2C(O)Me]_2[IrCl_6]$ and Its Os Analogue. *Eur. J. Inorg. Chem.* **2022**, *33*, No. e202200463.
(30) Sharutin, V. V.; Sharutina, O. K.; Senchurin, V. S.; Somov, N. V. Synthesis and structure of iridium complexes $[Ph_3PR][trans\text{-}IrCl_4(DMSO)_2]$. *Russ.J.Gen.Chem.* **2015**, *85*, 634−639.
(31) Warthmann, W.; Schmidt, A. Reaktionsprodukte aus Chlorsulfonium-Salzen und Alkoholen bzw. Wasser und deren IR-Spektren. *Chem. Ber.* **1975**, *108*, 520−527.
(32) Rudnitskaya, O. V.; Miroshnichenko, L. V.; Stash, A. I.; Sinitsyn, N. M. Synthesis and structure of trans-$[(DMSO)H][Ru(DMSO)_2Cl_2]$. *Zh. Neorg. Khim.* **1993**, *38*, 1187−1190.
(33) Alessio, E.; Santi, A. S.; Faleschini, P.; Calligaris, M.; Mestroni, G. New aspects of rhodium(III)−dimethyl sulfoxide chemistry: synthesis and molecular structure of $[NEt_4][cis\text{-}RhCl_4\{(CH_3)_2SO\}_2]$ and chemical behaviour in aqueous solution of $[RhCl_n\{(CH_3)_2SO\}_{6-n}]^{3-n}$($n$ = 3 or 4) complexes. *J. Chem. Soc. Dalton Trans.* **1994**, *13*, 1849−1855.
(34) Rudnitskaya, O. V.; Tereshina, T. A.; Dobrokhotova, E. V.; Kultyshkina, E. K.; Novikov, A. S.; Tskhovrebov, A. G.; Zubavichus, Y. V.; Khrustalev, V. N. Monoprotonated Dimethyl Sulfoxide, $[HOSMe_2]$+: Synthesis, Crystal Structure, Spectroscopic and Theoretical Studies of $[HOSMe_2]_2[OsCl_6] \cdot 2H_2O$. *ChemistrySelect* **2021**, *6*, 5211−5217.
(35) Gamage, S. N.; James, B. R.; Rettig, S. J.; Trotter, J. Synthesis and structural characterization of two triclinic modifications of diethylammonium trans-tetrachlorobis(dimethylsulfoxide-S)rhodate-(III): an example of hydrogen-bond acceptor structural isomerism. *Can. J. Chem* **1988**, *66*, 1123−1128.
(36) Song-Song, B.; Wang, Di.; Xin-Da, H.; Etter, M.; Cai, Z.-S.; Wan, X.; Dinnebier, R. E.; Zheng, L.-M. $Na_2Ir^{IV}Cl_6$: Spin−Orbital-Induced Semiconductor Showing Hydration-Dependent Structural and Magnetic Variations. *Inorg. Chem.* **2018**, *57*, 13252−13258.
(37) Rankin, D. A.; Penfold, B. R.; Fergusson, J. E. The chloro and bromo complexes of iridium(III) and iridium(IV). II. Structural chemistry of Ir(III) complexes. *Aust. J. Chem.* **1983**, *36*, 871−883.
(38) Coll, R. K.; Fergusson, J. E.; Penfold, B. R.; Rankin, D. A.; Robinson, W. T. The Chloro and Bromo Complexes of Iridium(III) and Iridium(IV). III. The Crystal-Structures of $K_3[IrCl_6]$ and $Cs_2[IrCl_5H_2O]$ and Interpretation of the N.Q.R. Data of Chloroiridates(III). *Aust. J. Chem.* **1987**, *40*, 2115−2122.
(39) Evans, P. Scaling and assessment of data quality. *Acta Crystallogr., Sect. D: Biol. Crystallogr.* **2006**, *62*, 72−82.
(40) Battye, T. G. G.; Kontogiannis, L.; Johnson, O.; Powell, H. R.; Leslie, A. G. W. iMOSFLM: a new graphical interface for diffraction-image processing with MOSFLM. *Acta Crystallogr., Sect. D: Biol. Crystallogr.* **2011**, *67*, 271−281.
(41) Winn, M. D.; Ballard, C. C.; Cowtan, K. D.; Dodson, E. J.; Emsley, P.; Evans, P. R.; Keegan, R. M.; Krissinel, E. B.; Leslie, A. G. W.; McCoy, A.; McNicholas, S. J.; Murshudov, G. N.; Pannu, N. S.; Potterton, E. A.; Powell, H. R.; Read, R. J.; Vagin, A.; Wilson, K. S. Overview of the CCP4 suite and current developments. *Acta Crystallogr.* **2011**, *D67*, 235−242.
(42) *Bruker, SAINT*, v. 8.34A; Bruker AXS Inc.: Madison, WI, 2014.
(43) Krause, L.; Herbst-Irmer, R.; Sheldrick, G. M.; Stalke, D. Comparison of silver and molybdenum microfocus X-ray sources for single-crystal structure determination. *J. Appl. Crystallogr.* **2015**, *48*, 3−10.
(44) Sheldrick, G. M. SHELXT − Integrated space-group and crystal-structure determination. *Acta Crystallogr., Sect. A: Found. Adv.* **2015**, *A71*, 3−8.
(45) Sheldrick, G. M. A short history of SHELX. *Acta Crystallogr., Sect. A: Found. Adv.* **2008**, *64*, 112−122.
(46) Sheldrick, G. M. Crystal structure refinement with SHELXL. *Acta Crystallogr.* **2015**, *C71*, 3−8.

https://doi.org/10.1021/acsomega.3c01012
ACS Omega 2023, 8, 20569−20578